

Research Article

River terraces along the Liujiang River in Southwest China and their implications for understanding fluvial processes on the Guizhou Plateau since the Late Pleistocene

Huan Qian^a , Xi Jiang^{a,b}, Hua Chen^a, Renchang Mi^a, Gary G. Lash^c and Huan Li^d 

^aCollege of Resources and Environmental Engineering, Key Laboratory of Karst Georesources and Environment, Ministry of Education, Guizhou University, Guiyang, Guizhou 550025, China; ^bGuizhou Karst Environmental Ecosystems Observation and Research Station, Guizhou University, Guiyang, Guizhou 550025, China;

^cDepartment of Geosciences, State University of New York, Fredonia, New York 14063, USA and ^dKey Laboratory of Metallogenic Prediction of Nonferrous Metals and Geological Environment Monitoring, Ministry of Education, School of Geosciences and Info-Physics, Central South University, Changsha, Hunan 410083, China

Abstract

River terraces serve as excellent indicators of the landform evolution of the Guizhou Plateau. This paper presents the results of terrace investigation and optically stimulated luminescence (OSL) dating focused on five sections along the Liujiang River of the southeastern Guizhou Plateau. The OSL ages of the terraces range from 0.21 ± 0.02 to 16.0 ± 1.4 ka for the first terraces (T1) and from 3.5 ± 0.3 to 26.5 ± 3.3 ka for the second terraces (T2), which are much younger than those of other basins on the Guizhou Plateau. These ages, considered in tandem with the results of previous investigations, enhance our understanding of the fluvial landform evolution of the Guizhou Plateau since the Late Pleistocene. On the Guizhou Plateau platform, terraces are considered to be the response of river evolution to tectonic uplift, indicating a relatively slow geomorphic process. In the slope zone, climate change has had a significant impact on the fluvial landform processes, driving the formation of the younger terraces along the Liujiang River. In the platform–slope transition zone, the evolution of terraces was driven by both tectonic uplift and climate change, where the landform processes were dominated by strong headward erosion.

Keywords: River terrace, OSL dating, geomorphic evolution, tectonic uplift, Guizhou Plateau

INTRODUCTION

Uplift of the Tibetan Plateau since the Late Cenozoic has been accompanied by the formation of three topographic regions in China. In their transition zones, the river dynamic process and development history has attracted the attention of numerous geomorphologists and geologists (e.g., Pan et al., 2012; Su et al., 2019; Yang et al., 2019; Liu F.L. et al., 2020; Liu Y.M., 2020; Wu C. et al., 2020; Liu Y.M. et al., 2022; Duan et al., 2023). The Guizhou Plateau is located in the second stepped topographic region of China, which is a transitional zone from the Tibetan Plateau to the Southeast Hills of China (Fig. 1A). Its geomorphic processes have also received extensive attention (e.g., Xu et al., 2013; Wang et al., 2015; Bai et al., 2019; Gao et al., 2020; Jiang M. et al., 2020; Yang et al., 2020; Fan et al., 2021).

Since Yang (1944) first proposed three physiographic stages of Guizhou landscape evolution, much debate has focused on the formation and evolution of multilevel planation surfaces on the Guizhou Plateau (e.g., Nie, 1994; Li X.Z., 2001; Cui et al., 2002; Li et al., 2002; Qin et al., 2002; Zhou et al., 2005; Li Z.F., 2011). But these debates are mostly qualitative analyses because of the lack of geochronological data. Therefore, Quaternary dating is

the most urgent scientific requirement for studying the geomorphic evolution of the Guizhou Plateau.

River terraces, the most prominent landforms present in montane valleys, provide abundant information about tectonic, climatic, and paleohydrologic changes (Starkel, 2003; Olszak, 2017; Liu et al., 2018; Schanz et al., 2018; Maddy et al., 2020). Owing to the staged alternating accumulation and erosion of river systems, terrace sediments not only record the evolution of the basin environment, but also provide excellent materials for geologic dating (Zhang et al., 2009; Gao et al., 2017; Delmas et al., 2018; Armas et al., 2019; Chauhan et al., 2023). Although terrace genesis and formation processes are disputed, the sedimentary attributes and geochronology of terrace sequences are especially useful for the reconstruction of river system development and geomorphic evolution (e.g., Kiden and Törnqvist, 1998; Finnegan and Dietrich, 2011; Bridgland and Westaway, 2014; Hu et al., 2016, 2019; Wu D.Y. et al., 2020; Wang et al., 2021).

On the Guizhou Plateau, terraces evolve from erosion terraces to fill terraces from west to east (Guizhou Geological Survey, 2018). The few ages for terrace T1 in the Huishui Basin and Caodu River obtained by use of ^{14}C methodology suggested that these terraces were largely formed in the Holocene (Gao et al., 1986; Lin et al., 1994). More recently, researchers have used optically stimulated luminescence (OSL) dating to study the terrace evolution and discuss the landform processes of intermontane basins since the Late Pleistocene, including the Chahe River (Hu, 2017), Wudang Basin (Jiang X. et al., 2020), Suiyang Basin

Corresponding author: X. Jiang; Email: xjiang@gzu.edu.cn

Cite this article: Qian H, Jiang X, Chen H, Mi R, Lash GG, Li H (2025). River terraces along the Liujiang River in Southwest China and their implications for understanding fluvial processes on the Guizhou Plateau since the Late Pleistocene. *Quaternary Research* 1–16. <https://doi.org/10.1017/qua.2024.44>



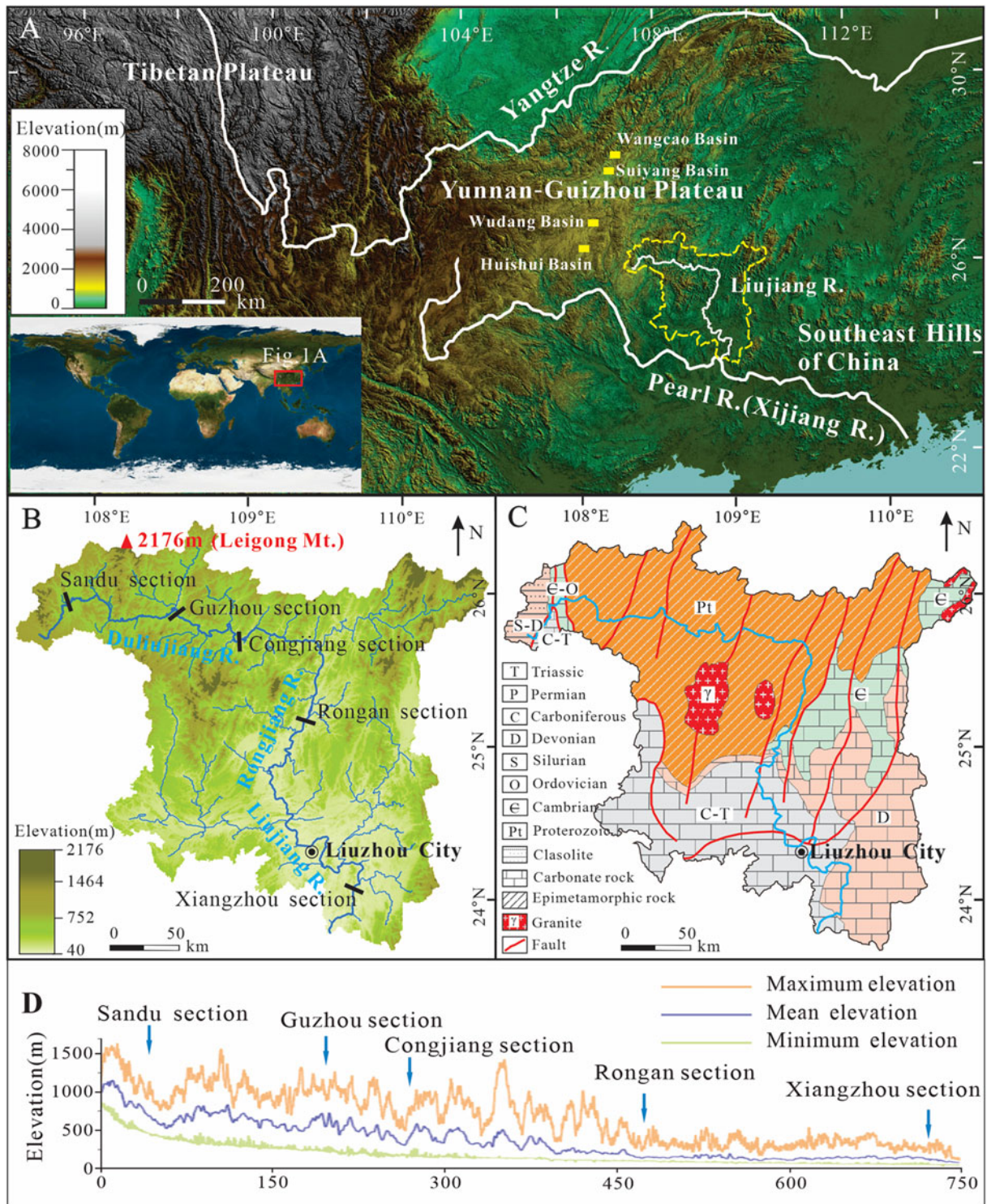


Figure 1. Geomorphological and geologic maps of the study area. (A) The basin of the Liujiang River, delineated by the yellow dashed line, is a geomorphic transition zone linking the Yunnan-Guizhou Plateau and Southeast Hills of China. (B) The main watercourse of the Liujiang River is divided into three regions from upstream to downstream, namely the Duliujiang River, Rongjiang River, and Liujiang River. The black short lines crossing the river indicate the locations of the studied five sections. (C) Geologic map of the Liujiang River basin based on the 1:500,000 regional geologic maps of Guizhou and Guangxi. (D) Topography along the Liujiang River as determined by swath profiles from an ASTER 30 m DEM (<https://www.gscloud.cn/>). The swath width on both sides of the river is 10 km. As is clear, the mean elevation shows that Sandu, Guzhou, and Congjiang in the upper reaches of the Liujiang River are located on the Guizhou Plateau, while Rongan and Xiangzhou in the lower reaches are located in the hills of northern Guangxi.

and Wangcao Basin (Jiang et al., 2021), Qingshuijiang River (Fan et al., 2022), and Huishui Basin (An et al., 2023). Terrace dating was also carried out on rivers originating from the plateau in the

first stepped topographic region adjacent to the Guizhou Plateau, including the Xijiang River (Yuan et al., 1988), Lishui River (Yang et al., 2011), and Yuanjiang River (Ren, 2019). However previous

research has mostly been scattered across small basins of various rivers, which has limited our understanding of the geomorphic processes driven by rivers of the Guizhou Plateau.

Here, we present the results of a terrace study based on the analysis of five sections along the Liujiang River, a river linking two topographic regions of the Guizhou Plateau and Southeast Hills of China. Developmental histories and ages of the terraces are based on field investigation and OSL dating. Our results combined with those of previous studies are used to discuss the timing and evolutionary dynamics of the river terraces on the Guizhou Plateau and provide new insights into the landform processes since the Late Pleistocene.

GEOMORPHOLOGICAL AND GEOLOGIC SETTING

The Liujiang River, with a total length of 773 km, is the second largest tributary of the Xijiang River, the main tributary of the Pearl River in China (Fig. 1A). The Liujiang River originates in Dushan County, Guizhou Province, and flows into the Xijiang River in Xiangzhou County, Guangxi Zhuang Autonomous Region. The upper reaches of the Liujiang River (from Dushan County, Guizhou, to Sanjiang County, Guangxi) are known as the Duliujiang River, whereas the middle reaches (from Sanjiang County, Guangxi, to Liucheng County, Guangxi) are referred to as the Rongjiang River. The lower reaches (from Liucheng County, Guangxi, to the confluence of the Xijiang River) are named the Liujiang River (Fig. 1B). The basin of the Liujiang River is located in the geomorphic transition zone between the Guizhou Plateau and the hills of northern Guangxi. The highest point of the basin is Leigong Mountain with an elevation of 2176 m, which is the main peak of the Miao Mountains on the Guizhou Plateau. The lowest point is located at the entrance of the Xijiang River at Xiangzhou, with an elevation of about 40 m. The upper reaches of the Liujiang River (Duliujiang River) are characterized by high mountains and deep valleys through which the river flows rapidly from west to east. The middle and lower reaches (Rongjiang River and Liujiang River, respectively) are characterized by low mountains and hills and wide river valleys through which water flows mainly from north to south (Fig. 1D).

The Liujiang River drainage basin is located in the Yangtze block. Upstream development of the river appears to have been largely influenced by the Rongjiang Caledonian open fold structure, whereas river development in the middle and downstream areas is mainly controlled by nearly north–south-trending fault structures (Guizhou Geological Survey, 2018). Strata in the upstream region from Dushan to Sandu mainly include Cambrian–Ordovician dolomite, Silurian–Devonian clastic, and Carboniferous–Triassic limestone (Fig. 1C). In the upper and middle reaches of the river, the main strata are Neoproterozoic metamorphic rocks, including metamorphic sandstone, metamorphic tuff, and slate. The main strata in the downstream region include Devonian to Triassic carbonate rocks.

METHODS

Field investigation and sampling

Field investigation was carried out along the main channel of the Liujiang River. Firstly, Google Earth images were used to identify potential locations of river terraces. We then surveyed these potential locations and only those valley sections hosting stable

and well-preserved terraces were considered for detailed field analysis. We identified five valley sections from the upstream to downstream segments of the Liujiang River, including the Sandu section, Guzhou section, Congjiang section, Rongan section, and Xiangzhou section (Fig. 1B). The poor preservation conditions of sediments in older terraces meant that only terraces T1 and T2 were investigated and dated in this work. We extracted the coordinates and elevation of the river terraces using a handheld GPS and ASTER DEM data with 30 m resolution (<https://www.gscloud.cn>), and sections were measured and sampled by use of a tape measure.

Samples to be dated were collected from sandy sediments in the terraces. Firstly, we excavated at least 30 cm of the surface layer on the profile to ensure that a sample represented original sediment. Then, a stainless steel pipe, 20 cm long and 5 cm in diameter, was hammered into the freshly exposed sandy layer. After the sample was filled, we immediately dug out the steel pipe and sealed it with a black plastic bag. When removing the steel pipe, the sediment around it was excavated and bagged for radiation background measurement. Generally, the sample was collected at a depth of about 1 m from the top of the terrace. For sedimentary profiles of an exposed thickness greater than 3 m, we excavated another sample at the bottom of the profile. We recovered 18 samples for dating from the five valley sections.

OSL dating

Geochronological analysis was carried out at the Qinghai Institute of Salt Lakes, Chinese Academy of Sciences. Only the sampled sand contained away from the end of the pipe and therefore less likely to have been exposed to light was removed from the sample pipe under the subdued red light of a darkroom. The sandy samples were first treated with 10% HCl and 30% H₂O₂ to remove carbonate and organic matter, respectively. After this, the wet-sieved grain-size fraction of 63–90 μm was etched with 40% HF for about 60 minutes to remove feldspar and eliminate the alpha-affected outer layer of the grains. Finally, extracted quartz grains were washed with 10% HCl to dissolve any fluoride precipitates, and the purity of the quartz samples was verified by infrared (IR) light (830 nm) stimulation. The IR stimulated luminescence (IRSL) detection method, based on the ratio of the luminescence signal stimulated by IR light to the luminescence signal stimulated by blue light (BL), was used to assess the quartz purity of the pre-treated sample. If the IR/BL ratio is less than 10%, it indicates that there is no significant IR signal in the sample. Any sample with an IR/BL ratio greater than 10% would be retreated again with HF to avoid equivalent dose (D_e) underestimation.

Luminescence signals were measured on a RisøTL/OSL-DA-20 automated system. A ⁹⁰Sr/⁹⁰Y beta source was used to provide the laboratory irradiation. The OSL signal of quartz was stimulated by blue LEDs ($\lambda = 470 \pm 20$ nm) at 130°C for 40 s, while the IR laser used to examine the feldspar component had a wavelength of 830 nm. The stimulated luminescence signals were recorded by a 9235QA photomultiplier tube after being filtered by a 7.5-mm-thick Hoya U-340 optical filter. During the testing process, the preheat temperature for the natural and regenerated doses was 260°C for 10 s, and the preheat temperature for the test dose was 220°C for 10 s. D_e measurement was conducted using a combination of the single-aliquot regenerative-dose (SAR) protocol and the standard growth curve (SGC) method, which has been widely used to determine the ages of different types of sediments (Mischke et al., 2017; Fan et al., 2022; Long

et al., 2022; Shen et al., 2022; An et al., 2023). The analytical procedure and data processing of the SAR-SGC method have been explained in detail by Long et al. (2022) and Shen et al. (2022).

The contents of U and Th were measured by inductively coupled plasma mass spectrometry (ICP-MS), and the content of K was measured by inductively coupled plasma optical emission spectrometry (ICP-OES). The cosmic ray dose rate was calculated considering the elevation, latitude, longitude, and burial depth of each sample (Prescott and Hutton, 1994). The annual dose can be calculated using the formulas and parameters provided by Aitken (1985), and the dose rate reported in this paper includes the contribution from cosmic radiation. The water content was assessed based on previous studies and actual measurements, and a uniform value of $10 \pm 5\%$ was chosen (Liu et al., 2021).

RESULTS

Sandu section

The Sandu section is located in the upstream region of the Duliujiang River (Fig. 1B). In this region, the Duliujiang River flows through a karst intermontane basin (Sandu Basin) with a relative height difference of more than 1000 m (Fig. 2A). Watershed strata are dominated by Cambrian–Ordovician dolomite. The region is characterized by large slopes and evidence of strong water erosion, and the carbonate bedrock is generally exposed along the river (Fig. 2B). Sediment in the river is dominated by gravel containing cobbles that exceed 50 cm in diameter. River terraces appear to have formed preferentially at river bends,

especially on convex banks. The terrace investigation at the Sandu section focused on two sedimentary profiles. Profile 1–1' (25.966°N, 107.862°E) is located in the downstream area of the Sandu Basin where terraces T2 and T1 are 25 and 15 m above the river level, respectively (Fig. 3A). Terrace T2 is a fill terrace consisting of a gravel layer and sandy layer (Fig. 3A). Terrace T1 in profile 2–2' (25.975°N, 107.840°E) is 6.3 m above the river level and consists, in bottom-up order, of dolomite basement, a gravel layer, and a sandy layer (Figs. 2B and 3B). Three OSL samples were collected from the Sandu section. The age of sample SD-01, which was recovered from a depth of 1.1 m in terrace T2 of profile 1–1', is 26.5 ± 3.3 ka (Figs. 2C and 3A). The ages of samples SD-02 and SD-03, which were collected from depths of 1.1 m and 3.2 m in terrace T1 of profile 2–2', are 6.1 ± 0.6 and 15.4 ± 1.8 ka, respectively (Figs. 2D and 3B).

Guzhou section

The Guzhou section is located in the middle reaches of the Duliujiang River (Fig. 1B). Strata in the watershed are dominated by Neoproterozoic metamorphic sandstone and metamorphic tuff and subordinate Upper Cretaceous conglomerate and siltstone distributed in the intermontane Rongjiang Basin. The Duliujiang River winds from west to east through the southern end of the basin (Fig. 4A). The area of the Guzhou section displays great elevation differences and evidence of strong fluvial erosion. River bends are commonly characterized by abundant coarse gravel on one side (Fig. 4B) and exposed bedrock on the other.

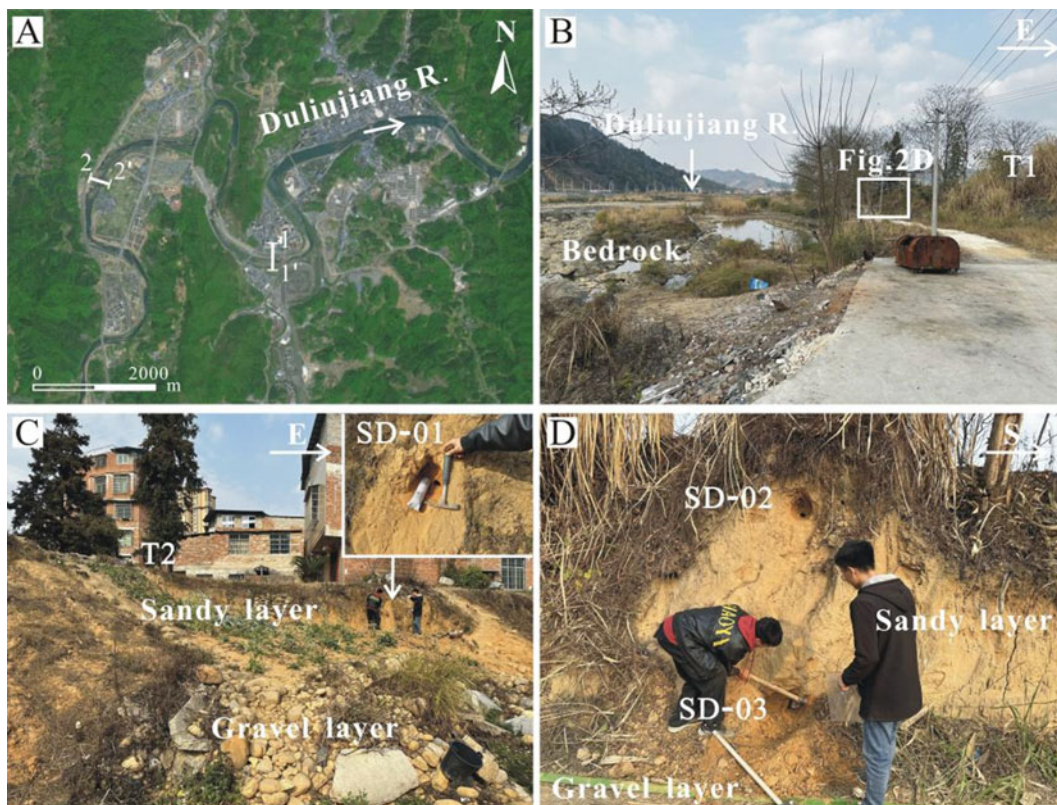


Figure 2. (A) Aerial photograph showing the location of the Sandu section in a karst intermountain basin. The Duliujiang River winds through the basin from west to east. The white line segments represent the locations of the terrace profiles shown in Figure 3A and B. (B) Field photograph displaying the strong erosion of exposed bedrock of the riverbed. The studied terrace was deposited on the convex bend of the river. (C) Location of sample SD-01 on terrace T2. (D) Locations of samples SD-02 and SD-03 on terrace T1.

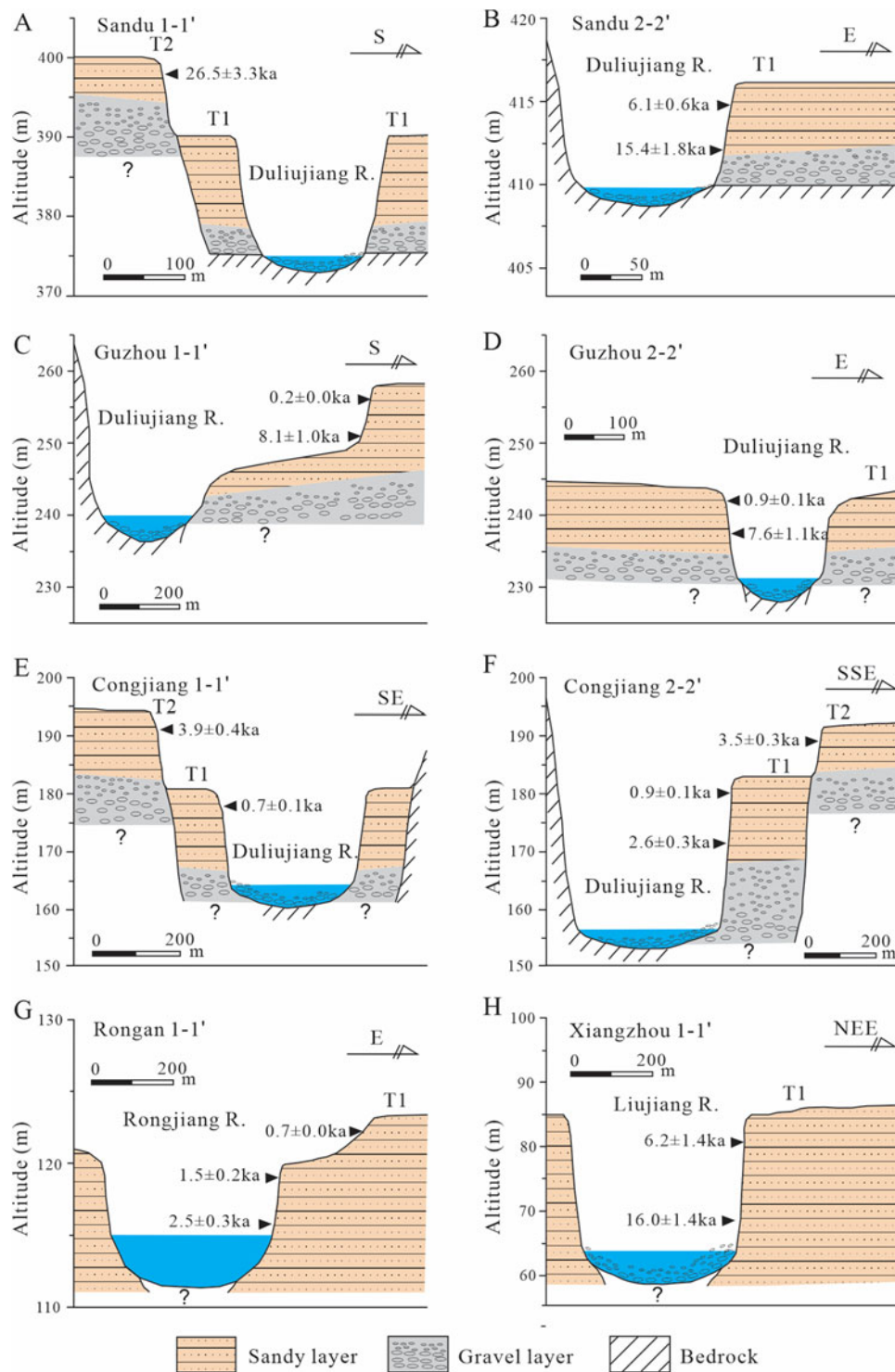


Figure 3. Sedimentary profiles of studied terraces along the Liujiang River. (A) Profile 1-1', Sandu section. (B) Profile 2-2', Sandu section. (C) Profile 1-1', Guzhou section. (D) Profile 2-2', Guzhou section. (E) Profile 1-1', Congjiang section. (F) Profile 2-2', Congjiang section. (G) Profile 1-1', Rongan section. (H) Profile 1-1', Xiangzhou section. Locations of the profiles are shown in Figures 2A, 4A, 5A, 6A, and 7A, respectively. The dating results of the terrace samples are detailed in Table 1.

Terrace T1 in the Guzhou section is 12 to 19 m above the river level. Terrace T2 is poorly preserved in the Guzhou section. Terrace T1 is a fill terrace containing an upper sandy layer greater than 5 m thick. Four OSL samples were collected from the Guzhou section. Samples RJ-01 and RJ-02, collected from depths

of 0.9 and 3.9 m from profile 1-1' (25.902°N, 108.506°E), have ages of 0.21 ± 0.02 and 8.1 ± 1.0 ka, respectively (Figs. 3C and 4C). Samples RJ-03 and RJ-04, recovered from profile 2-2' (25.916°N, 108.516°E) at depths of 0.8 and 3.8 m, have ages of 0.94 ± 0.11 and 7.6 ± 1.1 ka, respectively (Figs. 3D and 4D).

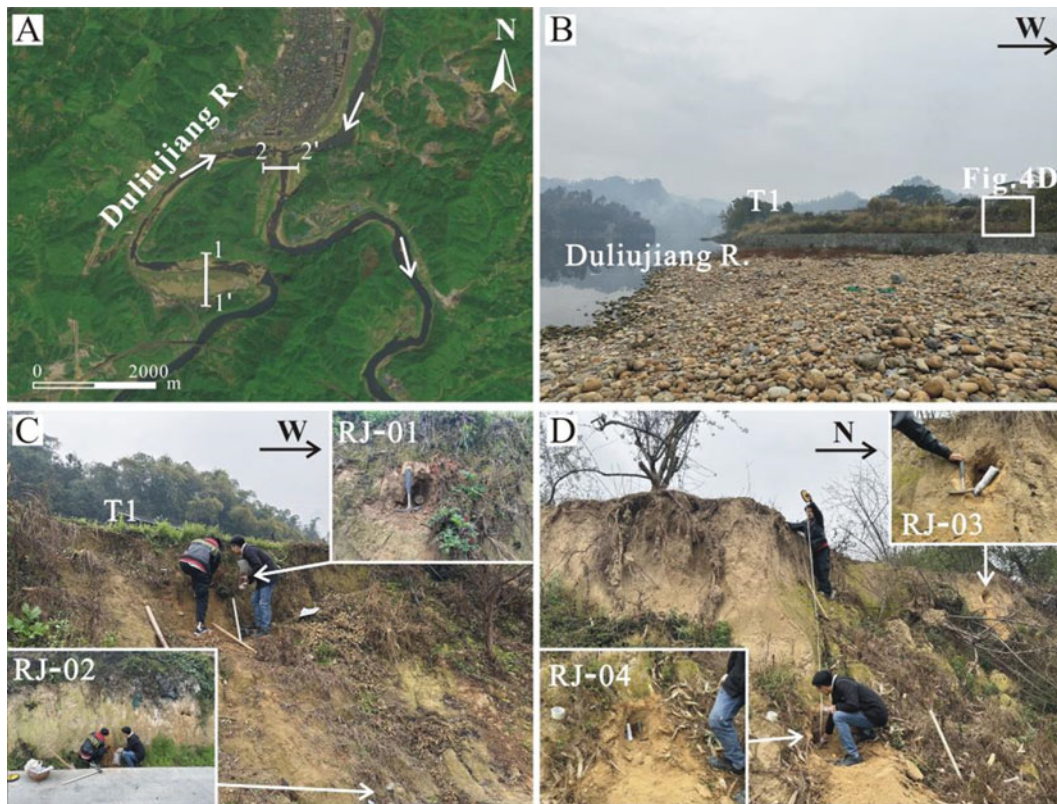


Figure 4. (A) Aerial photograph of the Duliujiang River flowing from west to east. The white line segments represent the locations of the terrace profiles illustrated in Figure 3C and D. (B) Terraces formed on the convex bends of the river where abundant coarse gravel accumulated. (C) Locations of samples RJ-01 and RJ-02 in profile 1–1'. (D) Locations of samples RJ-03 and RJ-04 in profile 2–2'.

Congjiang section

The Congjiang section is located in the lower reaches of the Duliujiang River (Fig. 1B). Bedrock of the watershed is mainly Neoproterozoic metamorphic rock. The Duliujiang River winds through the valley from west to east and experienced terrace formation at river bends (Fig. 5A). The riverbed at the Congjiang section contains more sediment and less exposed bedrock than at the Guzhou section. In addition to a thick gravel layer in the riverbed, a sandy layer accumulated in the convex bend of the river (Fig. 5B). We investigated two terrace profiles in the Congjiang section. Terraces T2 and T1 in profile 1–1' (25.697°N, 108.950°E) are 29 m and 16 m above the river level, respectively. Terraces T2 and T1 in profile 2–2' (25.715°N, 108.955°E) are 35 and 27 m above the river level, respectively. Terraces T1 and T2 are characterized by an upper sandy layer generally thicker than 10 m and an incompletely exposed lower gravel layer. Five OSL samples were collected from the terraces on the left and right banks of the Duliujiang River. Samples ML-01 and ML-02, excavated from a depth of 1.0 m in terraces T1 and T2 of profile 1–1', have ages of 0.67 ± 0.06 and 3.9 ± 0.4 ka (Figs. 3E, 5C, and 5D). Sample ML-03, which was recovered from a depth of 1.5 m in profile 2–2' in terrace T2, has an age of 3.5 ± 0.3 ka (Figs. 3F and 5E). Samples ML-04 and ML-05, collected from depths of 1.5 and 6.4 m (Fig. 5F) in profile 2–2' of terrace T1, have ages of 0.91 ± 0.08 and 2.6 ± 0.3 ka, respectively.

Rongang section

The Rongang section is located in Rongang County, Guangxi Autonomous Region, where the Rongjiang River flows from

north to south (Figs. 1B and 6A). Strata of the river valley are dominated by Cambrian carbonate rocks. The lack of bedrock exposed along the river likely reflects the flat terrain and related enhanced river sedimentation. The Rongang section is located in an intermontane basin characterized by a relative height difference of less than 500 m. The riverbed is not exposed because of impoundment induced by a downstream dam. Terrace T1 is about 9 m above river level. We did not find a stable gravel layer in terrace T1 except for scattered gravel exposed during excavation activities. Three OSL samples were collected from profile 1–1' (25.231°N, 109.407°E) (Fig. 3G). Sample RA-01, which was recovered from a depth of 0.5 m, has an age of 0.65 ± 0.05 ka (Fig. 6B). Samples RA-02 and RA-03, collected at depths of 1.0 and 4.1 m, have ages of 1.5 ± 0.2 and 2.5 ± 0.3 ka, respectively (Fig. 6C).

Xiangzhou section

The Xiangzhou section is located in the lower reaches of the north-to-south-flowing Liujiang River (Figs. 1B and 7A). Strata of this watershed are composed mainly of Devonian carbonate rocks. This region is characterized by hills and plains with an elevation range generally of less than 200 m. Sedimentation in this region dominated its geomorphic evolution resulting in the accumulation of abundant gravel and sand on both banks of the Liujiang River (Fig. 7B). Terraces are present on both sides of the river, and Quaternary sediment even covers some of the higher elevations. The inaccessibility of most of the terraces only permitted the investigation of terrace T1 of the Xiangzhou section. Terrace T1 in profile 1–1' (24.027°N, 109.684°E) is



Figure 5. (A) Aerial photograph of the Duliujiang River flowing through the Congjiang section. Terraces formed in bends of the river. The white line segments represent the locations of the terrace profiles illustrated in Figure 3E and F. (B) Gravels and sands are most abundant in the entry and export regions of the river bend. (C) Location of sample ML-02 in terrace T2, profile 1-1'. (D) Location of sample ML-01 excavated from terrace T1, profile 1-1'. (E) Location of sample ML-03 in terrace T2 bedding in profile 2-2'. (F) Locations of samples ML-04 and ML-05 collected from terrace T1, profile 2-2'.

about 21 m higher than the river level and is composed mainly of sand. Samples XZ-01, XZ-02, and XZ-03, which were recovered from depths of 1.4, 10.1, and 0.8 m to constrain the age of terrace T1, have ages of 6.2 ± 1.4 , 16.0 ± 1.4 , and 11.5 ± 1.0 ka, respectively (Figs. 3H, 7A, 7C, and 7D).

DISCUSSION

Ages of the terraces

Table 2 provides the dating results of previous studies of river terraces and layered caves on the Guizhou Plateau and neighboring areas. It must be emphasized that the terrace age is defined as the time of fluvial system transformation from deposition to incision (i.e., age of abandonment of the terrace), which is younger than the age of burial of the sediment at the terrace top. However, strong denudation of the Guizhou Plateau precludes the precise determination of terrace ages because of the dearth of reliable

dating materials. Therefore, our discussion is based on the burial ages of the sediments.

In previous studies, the ages of terraces T2 and T1 in the intermontane basins on the Guizhou Plateau platform mostly range from 57.4 to 177.4 ka and 8.0 to 35.1 ka, respectively, such as the Wudang Basin, Huishui Basin, and Suiyang Basin (Table 2, Fig. 8). The age differences in the same order terraces are more related to preservation conditions, the sedimentation process, and the depths of sample collection from the terraces and are less affected by regional structures. These terrace profiles mostly expose the bedrock base, a strath terrace, indicating that the terrain had undergone strong erosion. The similar age sequences and terrace types suggest that the fluvial landform evolution of the intermontane basins across the Guizhou Plateau has largely been synchronous since the Late Pleistocene.

The Guizhou Plateau is located in the core area of the South China Karst, where rivers cut down to not only form river terraces but also multilayer karst caves underground. Comparing these

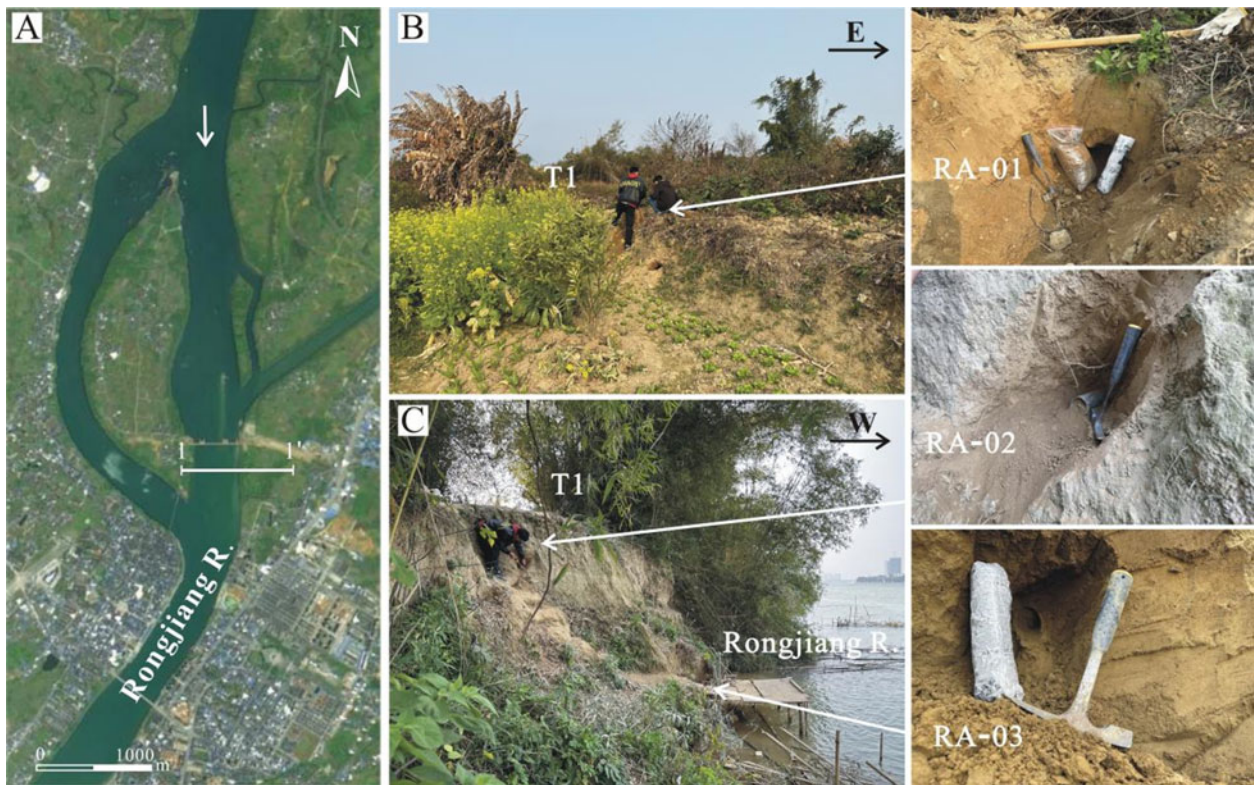


Figure 6. (A) Aerial image of the north-to-south-flowing Rongjiang River and the location of the Rongan section. The white line segment represents the location of the terrace profile illustrated in Figure 3G. (B) Location of sample RA-01 excavated from terrace T1. (C) Locations of samples RA-02 and RA-03 along the riverbank.

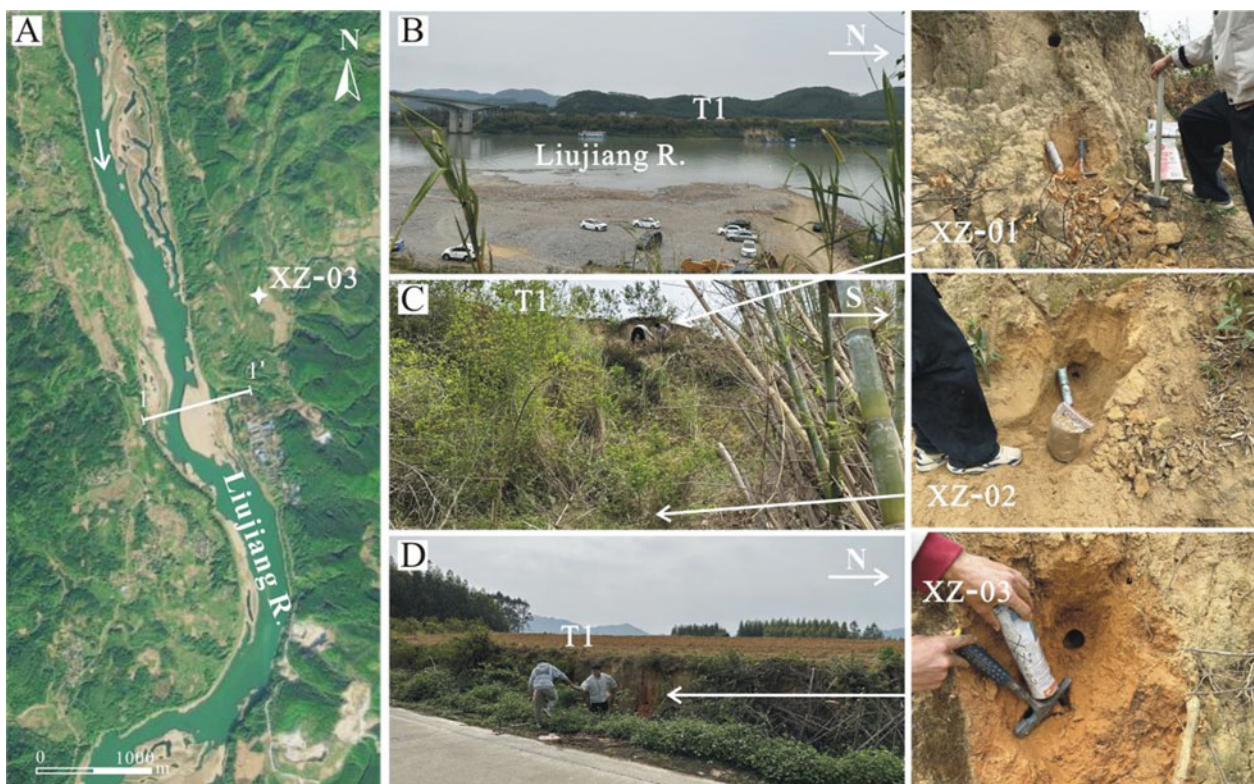


Figure 7. (A) Aerial image of the Liujiang River that flows through the Xiangzhou section from north to south. The white line segment represents the location of the terrace profile illustrated in Figure 3H. (B) Well-developed terraces along the riverbank. (C) Locations of samples XZ-01 and XZ-02 collected from terrace T1. (D) Location of sample XZ-03 collected from terrace T1.

Table 1. OSL dating results of the terraces along the Liujiang River

Sample ID	Depth (m)	K (%)	Th (ppm)	U (ppm)	Water content (%)	Dose rate (Gy/ka)	D _e (Gy)	Age (ka)
SD-01	1.1	0.35 ± 0.03	13.07 ± 0.70	2.29 ± 0.30	10 ± 5	1.69 ± 0.15	44.79 ± 4.09	26.5 ± 3.3
SD-02	1.1	0.73 ± 0.03	11.07 ± 0.70	2.30 ± 0.30	10 ± 5	1.88 ± 0.16	11.42 ± 0.55	6.1 ± 0.6
SD-03	3.2	0.55 ± 0.03	8.00 ± 0.60	1.71 ± 0.30	10 ± 5	1.39 ± 0.11	21.46 ± 1.80	15.4 ± 1.8
RJ-01	0.9	1.70 ± 0.04	15.63 ± 0.70	2.89 ± 0.30	10 ± 5	3.27 ± 0.22	0.69 ± 0.07	0.21 ± 0.02
RJ-02	3.9	1.58 ± 0.04	13.79 ± 0.70	2.74 ± 0.30	10 ± 5	2.95 ± 0.21	24.02 ± 2.50	8.1 ± 1.0
RJ-03	0.8	1.39 ± 0.04	12.66 ± 0.70	2.04 ± 0.30	10 ± 5	2.63 ± 0.19	2.48 ± 0.22	0.94 ± 0.11
RJ-04	3.8	0.91 ± 0.03	7.80 ± 0.60	1.46 ± 0.30	10 ± 5	1.71 ± 0.13	13.09 ± 1.59	7.6 ± 1.1
ML-01	1.0	1.16 ± 0.04	12.38 ± 0.70	2.06 ± 0.30	10 ± 5	2.41 ± 0.19	1.61 ± 0.06	0.67 ± 0.06
ML-02	1.0	1.70 ± 0.04	14.96 ± 0.70	2.45 ± 0.30	10 ± 5	3.13 ± 0.23	12.12 ± 1.07	3.9 ± 0.4
ML-03	1.5	1.46 ± 0.04	12.35 ± 0.70	2.09 ± 0.30	10 ± 5	2.66 ± 0.20	9.20 ± 0.47	3.5 ± 0.3
ML-04	1.5	1.35 ± 0.04	11.87 ± 0.70	1.77 ± 0.30	10 ± 5	2.47 ± 0.18	2.25 ± 0.09	0.91 ± 0.08
ML-05	6.4	1.23 ± 0.04	8.78 ± 0.70	1.65 ± 0.30	10 ± 5	1.93 ± 0.15	5.01 ± 0.30	2.6 ± 0.3
RA-01	0.5	1.38 ± 0.04	14.08 ± 0.70	2.65 ± 0.30	10 ± 5	2.85 ± 0.20	1.86 ± 0.04	0.65 ± 0.05
RA-02	1.0	1.80 ± 0.04	15.71 ± 0.70	2.98 ± 0.30	10 ± 5	3.37 ± 0.23	5.21 ± 0.48	1.5 ± 0.2
RA-03	4.1	1.49 ± 0.04	10.88 ± 0.70	2.02 ± 0.30	10 ± 5	2.53 ± 0.18	6.37 ± 0.70	2.5 ± 0.3
XZ-01	1.4	1.64 ± 0.04	12.53 ± 0.70	3.01 ± 0.30	10 ± 5	2.85 ± 0.20	17.77 ± 3.78	6.2 ± 1.4
XZ-02	10.1	1.40 ± 0.04	7.55 ± 0.60	1.71 ± 0.30	10 ± 5	1.98 ± 0.15	31.67 ± 1.27	16.0 ± 1.4
XZ-03	0.8	1.40 ± 0.04	13.10 ± 0.70	2.76 ± 0.30	10 ± 5	2.82 ± 0.22	32.52 ± 1.33	11.5 ± 1.0

karst caves with the terraces in the intermontane basins, it was found that the ages of the caves are only slightly older than those of the terraces, such as the second layered cave, L2, in the Suiyang Basin and the Nizhu River valley and the first layered cave, L1, in the Chahe River valley. These slight differences in age can be attributed to the fact that the ages of the layered caves were obtained by dating cave gravels, while the ages of the river terraces came from sandy sediments located above the gravel layers of the terraces, which leads to slightly older ages from the caves compared to those obtained from the river terraces. So we believe that the layered caves developed contemporaneously with the terraces in the intermontane basins.

OSL ages of terraces T2 and T1 of the Sandu Basin are 26.5 ka and 6.1–15.4 ka, respectively, which are comparable to terrace ages of the Wangcao Basin (Fig. 1) of northern Guizhou. In the Wangcao Basin, the age of terrace T2 at a depth of 3.6 m is 45.1 ka, and the age of T1 at a depth of 0.5 m is 5.5 ka (Jiang et al., 2021). As the Sandu and Wangcao basins are located in upstream regions of the rivers originating on the Guizhou Plateau, we propose that the development and geomorphic evolution of the terraces should be consistent in the Sandu and Wangcao basins. In the middle reaches of the Liujiang River, OSL ages of terrace T1 in the Guizhou and Rongan sections are less than 10 ka, and those of terraces T1 and T2 in the Congjiang section are less than 4 ka. For the Congjiang and Rongan section, the dates of sedimentation of T1 deposits differ among the studied terraces, yet downcutting appears to have occurred contemporaneously from 0.65 to 0.91 ka suggesting more rapid terrace evolution on the slope of the Guizhou Plateau. It is noteworthy that the Liujiang River as recorded in the Congjiang section appears to have experienced two rapid episodes of downcutting since 4 ka from T2 to T1. The ages of

terrace T1 in the Xiangzhou section are 6.2, 16.0, and 11.5 ka at depths of 1.4, 10.1, and 0.8 m, respectively. These ages are very close to T1 ages in terraces of the lower reaches of the Xijiang River (18.7 ka at a depth of 13 m) (Yuan et al., 1988) suggesting that the geomorphic evolution of downstream regions of the Liujiang River may have been contemporaneous with that of the Southeast Hills of China.

In summary, our dating results suggest that the ages of terraces along the Liujiang River are significantly younger than those on the Guizhou Plateau reflecting a more rapid river evolution process in the transition zone from the Guizhou Plateau to the hills of northern Guangxi.

Evolutionary dynamics of terraces

The dynamics of terrace formation, a long-standing focus of terrace research, can be attributed to climatic, tectonic, volcanic, and human activity (Finnegan and Dietrich, 2011; Olszak, 2017; Schanz et al., 2018; Maddy et al., 2020). According to classic geomorphological interpretation, terrace formation is related to the increase in the river channel gradient caused by tectonic uplift that induces downcutting of the river channel (Pan et al., 2009; Gao et al., 2017; Jia et al., 2017; Delmas et al., 2018). However, other studies maintain that climate change and the related changes in hydrodynamic conditions of the basin, including runoff, sediment supply, and even sea level, may play a role in terrace formation (Starkel, 2003; Pan et al., 2003; Bridgland and Westaway, 2008; Hu et al., 2017; Schanz et al., 2018). The Yellow River valley, northwest China, contains many well-preserved terraces because of the sealing effect of overlying loess layers. Age determinations of paleosols at the top of terraces suggest that river downcutting and terrace development occurred

Table 2. Dating results of terraces and layered caves on the Guizhou Plateau and neighboring areas

River system	Basin	Terrace/ layered cave	Elevation (m)	Height above river level (m)	Terrace type	Age (ka) ^a	Deposition rate ^b (m/ka)
Pearl River System	Sandu, Liujiang R. (this study)	T2	400	25	Fill terrace	26.5 ± 3.3 (OSL)	0.23
		T1	416	6.3	Strath terrace	6.1 ± 0.6 (OSL) 15.4 ± 1.8 (OSL)	
	Guzhou, Liujiang R. (this study)	T1	259	19	Fill terrace	0.21 ± 0.02 (OSL)	
		T1	243	12	Fill terrace	8.1 ± 1.0 (OSL) 0.94 ± 0.11 (OSL) 7.6 ± 1.1 (OSL)	0.45
	Congjiang, Liujiang R. (this study)	T2	194	29	Fill terrace	3.9 ± 0.4 (OSL)	2.88
		T1	181	16	Fill terrace	0.67 ± 0.06 (OSL)	
		T2	191	35	Fill terrace	3.5 ± 0.3 (OSL)	
		T1	183	27	Fill terrace	0.91 ± 0.08 (OSL) 2.6 ± 0.3 (OSL)	
	Rongan, Liujiang R. (this study)	T1	124	9	Fill terrace	0.65 ± 0.05 (OSL) 1.5 ± 0.2 (OSL) 2.5 ± 0.3 (OSL)	4.22
	Xiangzhou, Liujiang R. (this study)	T1	85	21	Fill terrace	6.2 ± 1.4 (OSL)	0.89
		T1	90	20	Fill terrace	16.0 ± 1.4 (OSL) 11.5 ± 1.0 (OSL)	
	Huishui Basin (An et al., 2023)	T2	930–960	10–20	Strath terrace	66.9 ± 3.8 (OSL)	0.04
		T1	920–955	3–10	Strath terrace	115.7 ± 11.0 (OSL) 122.4 ± 8.5 (OSL) 14.7 ± 1.3 (OSL) 31.2 ± 2.0 (OSL)	
Huishui Basin (Lin et al., 1994)	T1	920–955	~6	Strath terrace	8.010 ± 0.25 (¹⁴ C)		
Caodu R. (Lin et al., 1994)	T1	~700	5–10	Strath terrace	8.268 ± 0.14 (¹⁴ C)		
Libo (Liu Y. et al., 2022)	L2	575	10		560 ± 160 (TCN)		
Nizhu R. (Fan et al., 2021)	L2?	~1100	85		89.2 ± 0.3 (U-series)		
Chahe R. (Hu, 2017)	T2	~1800	110	Strath terrace	57.4 ± 5.7 (OSL)		
	T1	~1700	3	Strath terrace	61.6 ± 6.2 (OSL)		
	L1	1322	~25		35.1 ± 3.5 (OSL) 30.9 ± 3.1 (OSL)		
Yangtze River System	Liuchong R. (Liu Y. et al., 2022)	T2	1215	15	Strath terrace	410 ± 120 (TCN)	
	Qingshuijiang R. (Fan et al., 2022)	T2	~755	23	Strath terrace	51.1 ± 7.4 (OSL)	
		T1	~740	10	Strath terrace	25.5 ± 2.2 (OSL)	
		T2	~660	21	Strath terrace	57.7 ± 4.9 (OSL)	
		T2	~605	22	Strath terrace	122.3 ± 10.8 (OSL)	
		T2	~547	26	Strath terrace	102.3 ± 9.9 (OSL)	
	T1	~530	10	Strath terrace	103.5 ± 10.6 (OSL) 78.8 ± 6.3 (OSL)		
Suiyang Basin (Jiang et al., 2021)	T2	~862	10–14	Strath terrace	104.1 ± 7.2 (OSL)	0.06	
	T1	~855	3–6	Strath terrace/fill terrace	144.4 ± 10.7 (OSL) 8.2 ± 0.5 (OSL)	0.16	

Suiyang Basin (Yang et al., 2021)	L3	1130	90	16.7 ± 0.8 (OSL)
	L2	925	34	18.8 ± 1.1 (OSL)
Wangcao Basin (Jiang et al., 2021)	T2	690	20	320 ± 90 (TCN)
	T1	680	10	180 ± 90 (TCN)
Wudang Basin (Jiang X. et al., 2020)	T2	~1015	15–18	45.1 ± 3.2 (OSL)
	T1	~1000	2–5	5.5 ± 0.3 (OSL)
Yuanjiang R. (Ren, 2019)	T3	~180	~23	87.6 ± 6.8 (OSL)
	T2	~171	~14	114.0 ± 11.9 (OSL)
Lishui R. (Yang et al., 2011)	T3	~152	~30	177.4 ± 17.0 (OSL)
	T2	~140	~18	26.7 ± 1.8 (OSL)
	T3	230–235	25–62	23.6 ± 1.8 (OSL)
	T2	206	15–33	154.9 ± 15 (ESR)
	T3			70.6 ± 7 (ESR)
	T2			178.7 ± 15 (ESR)
	T3			109.5 ± 10 (ESR)
	T2			104.45 ± 8.88 (TL)
	T3			117.62 ± 9.99 (TL)
	T2			151.05 ± 12.84 (TL)
	T3			201.24 ± 17.11 (TL)
	T2			60.95 ± 5.18 (TL)

^aAbbreviations in brackets after ages represent the dating methods: TCN, terrestrial cosmogenic nuclide; ESR, electron spin resonance; TL, thermoluminescence.

^bCalculated on the same profile by dividing the height difference between two samples by their difference in age.

largely during the transition from glacial to interglacial climates, consistent with hypotheses of terrace formation that involve climate change (e.g., Pan et al., 2003, 2009; Gao et al., 2016; Hu et al., 2016, 2019).

Figure 9 presents the ages of terraces on the Guizhou Plateau and the history of climate change recorded by marine isotope stages (MIS) since 200 ka. It is shown that for the strath terraces on the platform of the Guizhou Plateau, such as the Wudang Basin, Huishui Basin, and Suiyang Basin (Fig. 1), the sedimentation history spans several climatic stages and the undercutting of terraces does not seem to be related to glacial–interglacial climate transition. So climate change may not be the primary driver for the formation of these terraces.

Tectonic uplift has been the main dynamic background process of the Guizhou Plateau since Quaternary time. On the plateau platform (elevation of about 700–1500 m), four strath terraces display a robust correlation with four layered karst caves in the Guizhou Plateau (Gao et al., 1986; Guizhou Geological Survey, 2018). Explanations of terrace development as a consequence of climate change hold that terrace formation is induced by changes in the amount of sediment transported by rivers, which results in periodic accumulation and erosion of sediment. This process appears to have been active in the Yellow River valley, presumably due to the more significant impact of changes in sediment content of the river on the loose semi-consolidated silty and muddy bedrock of the basin. However, on the Guizhou Plateau with hard carbonate strata, if there was only a change in water flow caused by climate change without a significant fall in erosion base level in the watershed caused by tectonic uplift, it seems impossible for the underground river (water-filled caves) to rapidly downcut through tens of meters thick rock beds (forming multilayered caves). Therefore, considering the good coupling of the development relationship between the terraces and the layered karst caves, we suggest that tectonic uplift was the main driving force for the formation of river terraces on the platform of the Guizhou Plateau.

River terraces on the slope zone that separates the Guizhou Plateau from the northern Guangxi hills and contains the Guizhou, Congjiang, and Rongnan sections along the Liujiang River, display significantly different developmental characteristics from terraces on the plateau platform. Firstly, the former terraces are fill terraces that contain very thick sandy layers. Moreover, their ages are significantly younger than those of terraces on the plateau platform, reflecting the effects of very rapid sedimentary and erosion processes. Results of the present study (Table 2) indicate that the ages of the top of terrace T1 are generally in the range of 0.65 to 0.94 ka. The ages of terrace T2 in the Congjiang section are 3.5 and 3.9 ka. Comparison of the ages of these terraces with high-precision paleoclimate records obtained from the analysis of a stalagmite in Dongge Cave within the Liujiang River watershed (Dykoski et al., 2005) suggests that the formation of the terraces T1 and T2 seems to be related to two centennial-scale climate events (Fig. 10). In the paleoclimate records of the stalagmite, two significant periods of climate change occurred at 707 yr BP and 3550 yr BP, respectively, which may have caused hydrodynamic changes in the nearby Liujiang River. The abrupt event of ~3.5 ka has also been found in different climatic records from around the world (e.g., Bond et al., 2001; Haug et al., 2001; Fleitmann et al., 2003; Dykoski et al., 2005). We posit, then, that on the slope of the Guizhou Plateau, rapid sediment accumulation and fluvial downcutting related to climate change may have been the reason for the

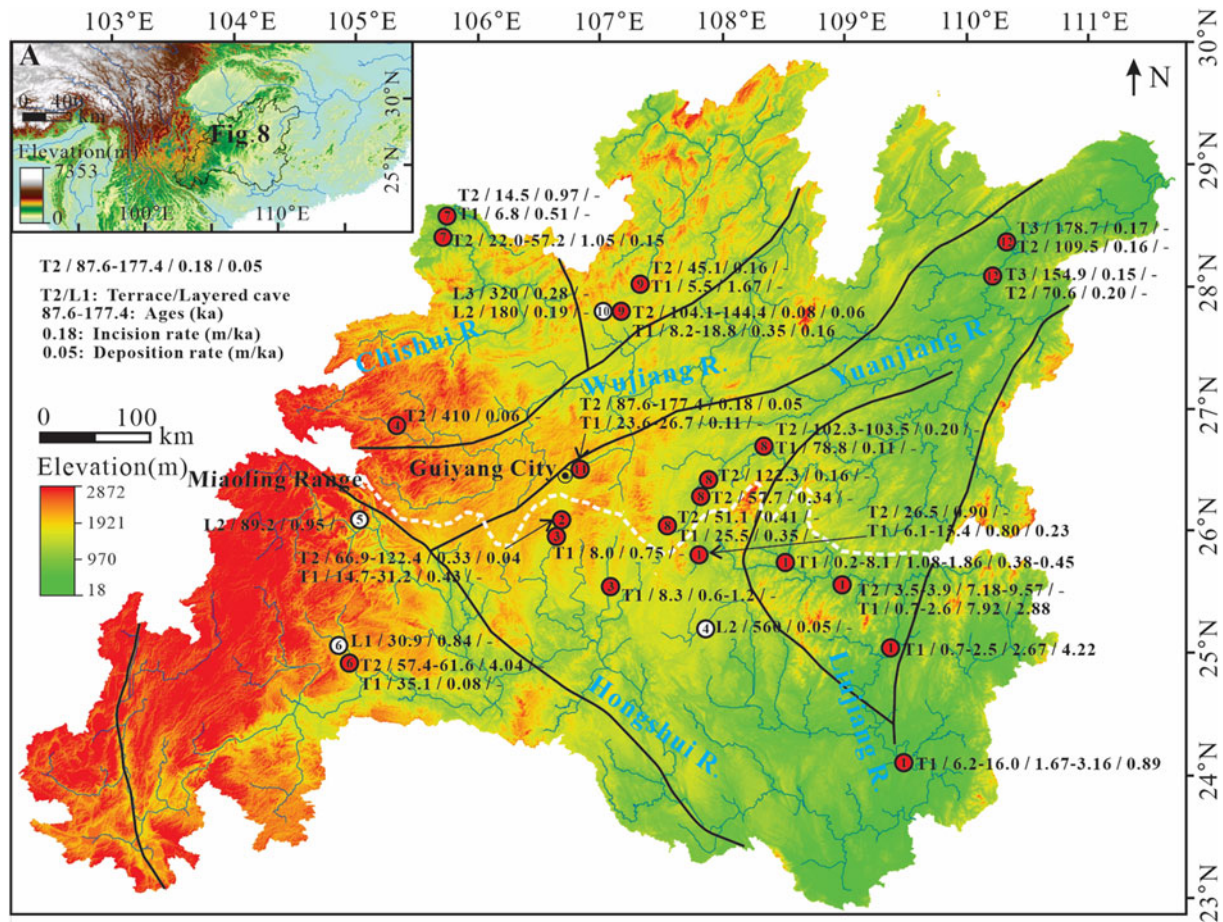


Figure 8. Map illustrating the main rivers originating on the Guizhou Plateau and dating results of terraces and layered caves along these rivers. Black lines denote faults. Red and white filled circles represent river terraces and layered caves, respectively. Numbers in the circles indicate data sources: 1 = this study; 2 = An et al. (2023); 3 = Lin et al. (1994); 4 = Liu Y. et al. (2022); 5 = Fan et al. (2021); 6 = Hu (2017); 7 = unpublished study by the authors; 8 = Fan et al. (2022); 9 = Jiang et al. (2021); 10 = Yang et al. (2021); 11 = Jiang X. et al. (2020); 12 = Ren (2019).

formation of the fill terraces documented along the Liujiang River, and these climate changes did not form terraces on the platform of the Guizhou Plateau, possibly due to the less sensitive response of fluvial adjustments to climate change in the platform area compared to rivers in the slope zone.

Terrace formation in the Sandu and Wangcao basins in the transition zone from the platform to the slope of the Guizhou Plateau may reflect the combined effects of tectonic uplift and climate change. Like the basins on the plateau platform, the geomorphic evolution in the basins of the transition zone was likely strongly affected by tectonic uplift of the Guizhou Plateau resulting in terraces with exposed bedrock. The basins of the transition zone are located upstream of the rivers originating on the Guizhou Plateau and affected by strong headward erosion. Rapid and unstable water flow related to climate change made these basins prone to channel adjustments that resulted in the formation of fill terraces.

Implications for landform evolution of the Guizhou Plateau

The results of our analysis of the ages and evolutionary dynamics of the studied terraces permit the division of the Guizhou Plateau into four subunits, each characterized by unique fluvial landform processes since Late Pleistocene time.

The plateau platform comprises the main area of the Guizhou Plateau, with an elevation range from about 700 to 1500 m, decreasing gradually from west to east. More than 70% of karst caves in the Guizhou Plateau are found in this subunit (Zhou et al., 2017) where they display a strong developmental association with the terraces of such intermontane basins as the Wudang, Huishui, and Suiyang basins (Table 2, Fig. 8). There are mainly strath terraces with low and stable heights above river level. Both terraces T1 and T2 had experienced stable sedimentation, especially T2, for as much as tens of thousands of years. Tectonic uplift appears to have been the main driving force for terrace development in this subunit, resulting in a terrace evolution characterized by low deposition and incision rates, favoring relatively slow landform processes. Although the Yuanjiang River basin is located on the slope of the Guizhou Plateau, its terrace evolution appears consistent with that of the plateau platform due to its gentle gradient and mild terrain.

The platform–slope transition zone is located on the edge of the plateau platform and is characterized by an elevation range of about 400 to 700 m. The Sandu and Wangcao basins are included in the platform–slope transition zone (Table 2, Fig. 8). Strath and fill terraces display varying heights above river level. In the upstream location of this subunit, rapid water system adjustments often occur, resulting in poorly developed karst

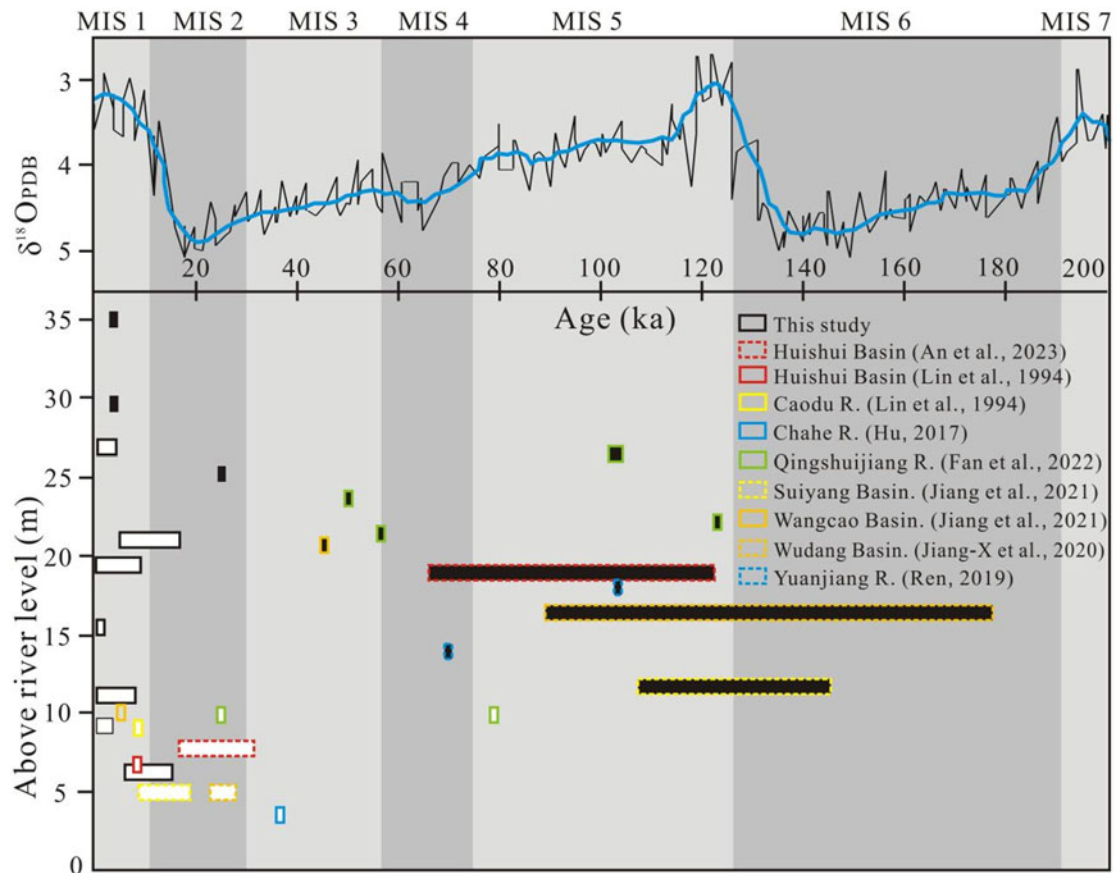


Figure 9. Comparison of ages of terraces on the Guizhou Plateau relative to the 200 ka record of climate change recorded by marine isotope stages (MIS). MIS data and the division are from Zachos et al. (2001). The black and white filled terrace ages represent terraces T2 and T1, respectively.

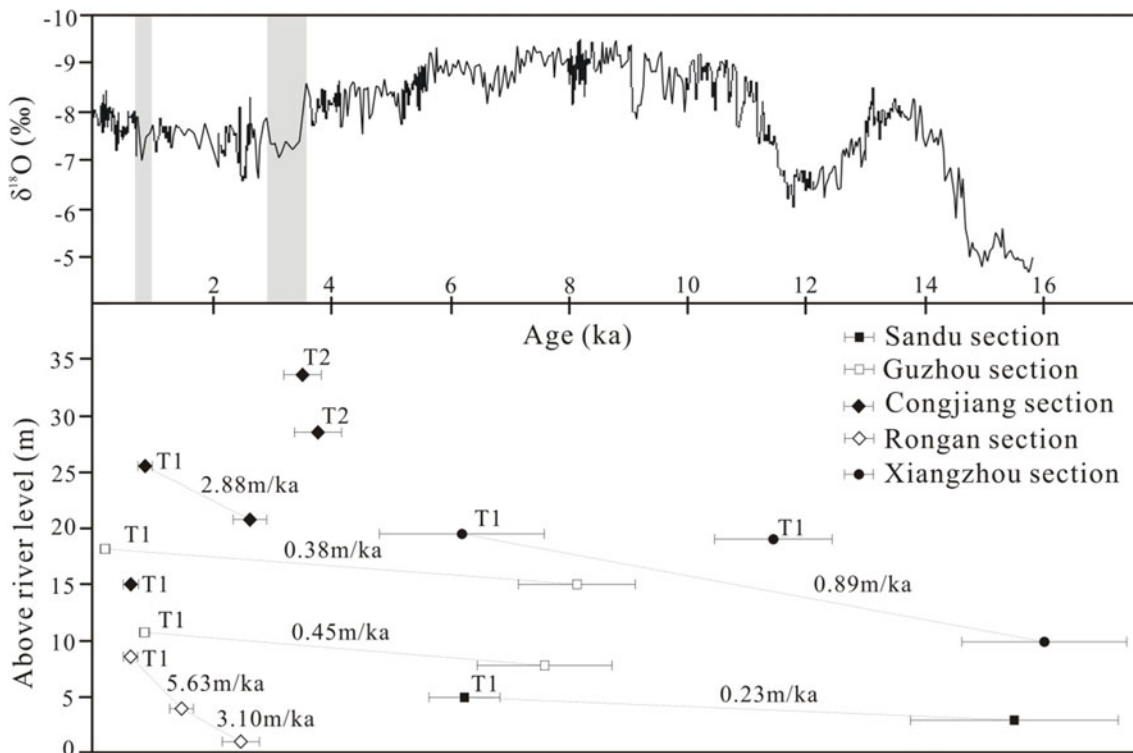


Figure 10. Comparison of the timing of terrace formation along the Liujiang River and the climate record obtained from the analysis of a stalagmite in Dongge Cave (Dykoski et al., 2005). Numerical values in the figure are deposition rates of the terraces (shown in Table 2 and Fig. 8).

caves (Zhou et al., 2017). The dual effects of tectonic uplift and climate change in the platform–slope transition zone mean that terraces form more quickly here than on the plateau platform. Landform processes in the platform–slope transition zone are dominated by strong headward erosion of bedrock by rivers.

The plateau slope (elevation of 200 to 600 m) is characterized by the convergence of tributaries and upstream channels into the main trunk of the Liujiang River. Ample water flow and an elevated topographic gradient mean that rivers have a very strong impact on landscape transformation in this subunit. The plateau slope exhibits the most rapid evolution of terraces on the Guizhou Plateau and includes the Guzhuo, Congjiang, and Rongan sections along the Liujiang River. Young fill terraces formed along the river in response to abrupt climate changes. These terraces display varying heights above river level as well as evidence of very high sedimentation and incision rates (Table 2, Fig. 8).

The slope–plain subunit is located in the first stepped topographic region adjacent to the Guizhou Plateau where the elevation is generally less than 300 m (Fig. 8). The Xiangzhou section of the Liujiang River and the Chishui River valley are found in the slope–plain subunit. The generally flat terrain and large runoff of this subunit mean that fluvial landform process are dominated by sedimentation. Tectonic displacement and climate change favored the widespread development of loose fill terraces along the rivers that exhibit evidence of rapid deposition and incision rates (Table 2, Fig. 8).

CONCLUSIONS

Field investigation and OSL dating were conducted on terrace deposits of five sections along the Liujiang River. We combine our results regarding the ages, dynamics, and geomorphic significance of the studied terraces with results of previous investigations of other terraces on the Guizhou Plateau. The main conclusions can be summarized as follows.

Terraces T1 and T2 along the Liujiang River are mainly fill terraces that become thicker in the downstream direction. Terrace ages range from 0.21 ± 0.02 to 16.0 ± 1.4 ka for T1 and 3.5 ± 0.3 to 26.5 ± 3.3 ka for T2.

Terraces of the Liujiang basin are characterized by greater deposition and incision rates than those of the Wudang, Huishui, and Suiyang basins, suggesting more rapid river evolution in the transition zone from the Guizhou Plateau to the hills of northern Guangxi.

The impact of climate on terrace evolution in the Liujiang River basin is much more significant than that on the platform of the Guizhou Plateau where terrace formation appears to have been controlled by staged tectonic uplift. Climate change was the main driving force for rapid accumulation and downcutting of the terraces in the middle section of the Liujiang River.

The Guizhou Plateau comprises four subunits of differing fluvial landform processes that have been active since at least Late Pleistocene time. The plateau platform has experienced relatively slow landform processes driven by tectonic uplift. In the platform–slope transition zone, the landform processes are mainly dominated by strong headward erosion, where the terrace evolution was affected by tectonic uplift and climate change. The plateau–slope region experienced the fastest fluvial landform evolution on the Guizhou Plateau. Terrace development on the plateau slope responded quickly to climate change. The slope–plain subunit is dominated by widespread and rapid

sedimentation. Terrace development was most influenced by the combination of tectonic movement and climate change.

Acknowledgments. We thank Dr Yixuan Wang for experiment assistance with OSL dating. This study was financially supported by the National Natural Science Foundation of China (Grant No.: 42061002) and Science and Technology Foundation of Guizhou Province (Grant No.: [2019]2852, [2020]1Y164).

Data availability. Data presented in this manuscript are available on request.

Competing interests. The authors declare that they have no known competing financial interests or personal relationships that could have appeared to influence the work reported in this paper.

References

- Aitken, M.J., 1985. *Thermoluminescence Dating*. Academic Press, London.
- An, N., Jiang, X., Qian, H., Chen, W.Q., Ning, F., Chen, H., Qin, N.X., Zhou, Y., 2023. River terrace characteristics and their geomorphic significance in Huishui Basin along Lianjiang River in Guizhou Plateau. [In Chinese with English abstract.] *Geological Review* **69**, 2023020028. <https://doi.org/10.16509/j.georeview.2023.04.002>.
- Armas, L., Necea, D., Miclaus, C., 2019. Fluvial terrace formation and controls in the Lower River Danube, SE Romania. *Quaternary International* **504**, 5–23.
- Bai, Y.E., Liu, Q., Gu, Z.F., Lu, Y.R., Sheng, Z.P., 2019. The dissolution mechanism and karst development of carbonate rocks in karst rocky desertification area of Zhenfeng-Guanling-Huaijiang County, Guizhou, China. *Carbonates & Evaporites* **34**, 45–51.
- Bond, G., Kromer, B., Beer, J., Muscheler, R., Evans, M.N., Showers, W., Hoffmann, S., Lotti-Bond, R., Hajdas, I., Bonani, G., 2001. Persistent solar influence on North Atlantic climate during the Holocene. *Science* **294**, 2130–2136.
- Bridgland, D.R., Westaway, R., 2008. Climatically controlled river terrace staircases: a worldwide Quaternary phenomenon. *Geomorphology* **98**, 285–315.
- Bridgland, D.R., Westaway, R., 2014. Quaternary fluvial archives and landscape evolution: a global synthesis. *Proceedings of the Geologists' Association* **125**, 600–629.
- Chauhan, N., Sundriya, Y., Kaushik, S., Chahal, P., Panda, D.K., Banerjee, D., Narayanan, A., Shukla, A.D., 2023. Chronology and paleoclimatic implications of the upper Ganga catchment floods since Marine Isotopic Stage-2. *Palaeogeography, Palaeoclimatology, Palaeoecology* **620**, 111566. <https://doi.org/10.1016/j.palaeo.2023.111566>.
- Cui, Z.J., Li, D.W., Feng, J.L., Liu, G.N., Li, H.J., 2002. The covered karst, weathering crust and karst (double level) planation surface. *Science in China (Series D)* **45**, 366–379.
- Delmas, M., Calvet, M., Gunnell, Y., Voinchet, P., Manel, C., Braucher, R., Tissoux, H., Bahain, J.J., Perrenoud, C., Saos, T., 2018. Terrestrial ^{10}Be and electron spin resonance dating of fluvial terraces quantifies quaternary tectonic uplift gradients in the eastern Pyrenees. *Quaternary Science Reviews* **193**, 188–211.
- Duan, M.Y., Neubauer, F., Robl, J., Zhou, X.H., Liebl, M., Argentin, A.L., Dong, Y.P., et al., 2023. Northeastward expansion of the Tibetan Plateau: topographic evidence from the North Qinling Mts.–Weihe Graben Coupling system, Central China. *Palaeogeography, Palaeoclimatology, Palaeoecology* **623**, 111612. <https://doi.org/10.1016/j.palaeo.2023.111612>.
- Dykoski, C.A., Edwards, R.L., Cheng, H., Yuan, D.X., Cai, Y.J., Zhang, M.L., Qing, J.M., An, Z.S., Revenaugh, J., 2005. A high-resolution, absolute-dated Holocene and deglacial Asian monsoon record from Dongge Cave, China. *Earth and Planetary Science Letters* **233**, 71–86.
- Fan, Y.L., Liu, J.J., Zhu, K.W., Li, H.B., Zou, X.X., 2021. Study on river downcutting rate in karst canyon: a case study of Nizhu River Grand Canyon in Beipan River. [In Chinese with English abstract.] *Quaternary Sciences* **41**, 1558–1564.
- Fan, Y.L., Wang, Y.X., Luo, G.J., Ren, D.Y., Li, Z.M., Liu, F.L., Luo, X.Q., Tang, L., Bai, Q.L., Li, C.D., 2022. The development of terraces and the

- implications for the geomorphologic evolution of the Qingshuijiang River in Guizhou Plateau since the Late Pleistocene. [In Chinese with English abstract.] *Scientia Geographica Sinica* **42**, 1676–1684.
- Finnegan, N.J., Dietrich, W.E.**, 2011. Episodic bedrock strath terrace formation due to meander migration and cutoff. *Geology* **39**, 143–146.
- Fleitmann, D., Burns, S.J., Mudelsee, M., Neff, U., Kramers, J., Mangini, A., Matter, A.**, 2003. Holocene forcing of the Indian Monsoon recorded in a stalagmite from southern Oman. *Science* **300**, 1737–1739.
- Gao, D.D., Zhang, S.C., Bi, K., Sheng, X.Y., Dong, C.Z., Wu, Z.M., Nie, Y.P.**, 1986. *Karst in South Guizhou, China*. [In Chinese.] Guizhou People's Publishing House, China.
- Gao, H.S., Li, Z.M., Ji, Y.P., Pan, B.T., Liu, X.F.**, 2016. Climatic and tectonic controls on strath terraces along the upper Weihe River in central China. *Quaternary Research* **86**, 326–334.
- Gao, H.S., Li, Z.M., Liu, X.F., Pan, B.T., Wu, Y.J., Liu, F.L.**, 2017. Fluvial terraces and their implications for Weihe River valley evolution in the Sanyangchuan Basin. *Science China Earth Sciences* **60**, 413–427.
- Gao, Q.S., Wang, S.J., Peng, T., Peng, H.J., Oliver, D.M.**, 2020. Evaluating the structure characteristics of epikarst at a typical peak cluster depression in Guizhou plateau area using ground penetrating radar attributes. *Geomorphology* **364**, 107015. <https://doi.org/10.1016/j.geomorph.2019.107015>.
- Guizhou Geological Survey**, 2018. *Regional Geology of Guizhou Province (Book 2)*. [In Chinese.] Geological Publishing House, Beijing, pp. 1117–1151.
- Haug, G.H., Hughen, K.A., Sigman, D.M., Peterson, L.C., Rohl, U.**, 2001. Southward migration of the intertropical convergence zone through the Holocene. *Science* **293**, 1304–1308.
- Hu, C.S., Liu, S.C., Hu, C.Q., Xu, G.L., Zhou, Y.Q.**, 2017. Fluvial incision by the Qingyijiang River on the northern fringe of Mt. Huangshan, eastern China: responses to weakening of the East Asian summer monsoon. *Geomorphology* **299**, 85–93.
- Hu, Z.B., Li, M.H., Dong, Z.J., Guo, L.Y., Bridgland, D., Pan, B.T., Li, X.H., Liu, X.F.**, 2019. Fluvial entrenchment and integration of the Sanmen Gorge, the Lower Yellow River. *Global and Planetary Change* **178**, 129–138.
- Hu, Z.B., Pan, B.T., Guo, L.Y., Vandenberghe, J., Hu, X.F.**, 2016. Rapid fluvial incision and headward erosion by the Yellow River along the Jinshaan gorge during the past 1.2 Ma as a result of tectonic extension. *Quaternary Science Reviews* **133**, 1–14.
- Hu, Z.D.**, 2017. *Active Tectonic and its Influence on Geomorphology in Xingyi, Guizhou*. [In Chinese.] Master's thesis, Chengdu University of Technology, Chengdu.
- Jia, L.Y., Hu, D.G., Wu, H.H., Zhao, X.T., Chang, P.Y., You, B.J., Zhang, M., et al.**, 2017. Yellow River terrace sequences of the Gonghe-Guide section in the northeastern Qinghai-Tibet: implications for plateau uplift. *Geomorphology* **295**, 323–336.
- Jiang, M., Lin, Y., Chan, T.O., Yao, Y.J., Zheng, G., Luo, S.Z., Zhang, L., Liu, D.P.**, 2020. Geologic factors leadingly drawing the macroecological pattern of rocky desertification in southwest China. *Scientific Reports* **10**, 1440. <https://doi.org/10.1038/s41598-020-58550-1>.
- Jiang, X., Chen, W.Q., Ning, F., Sun, Y.H., Ao, J., Luo, W.J., Kuang, G.X.**, 2021. River terraces in the northern Guizhou Plateau and their implications for karst landform evolution. [In Chinese with English abstract.] *Geographical Research* **40**, 81–92.
- Jiang, X., Chen, W.Q., Ning, F., Zheng, J., Luo, W.J., Zhou, Y.**, 2020. Sediment characteristics of terraces in Wudang Basin and their implications on basin evolution. [In Chinese with English abstract.] *Geographical Research* **39**, 1242–1254.
- Kiden, P., Törnqvist, T.E.**, 1998. Can river terrace flights be used to quantify Quaternary tectonic uplift rates? *Journal of Quaternary Science* **13**, 573–575.
- Li, D.W., Cui, Z.J., Liu, G.N.**, 2002. A development model of red weathering crust on limestones: an example from Hunan, Guangxi, Guizhou, Yunnan and Tibet. [In Chinese with English abstract.] *Acta Geographica Sinica* **57**, 293–300.
- Li, X.Z.**, 2001. Evolution of karst geomorphology of Upper-Cenozoic and its influential factors in Guizhou Plateau. [In Chinese with English abstract.] *Guizhou Geology* **18**, 29–36.
- Li, Z.F.**, 2011. Division of karst landform in Guizhou. [In Chinese with English abstract.] *Guizhou Geology* **28**, 177–182.
- Lin, S.J., Zhou, Q.Y., Chen, P.Y.**, 1994. *Late Cenozoic of Guizhou*. [In Chinese.] Guizhou Science and Technology Press, Guiyang, China, pp. 88–101.
- Liu, F.L., Gao, H.S., Li, Z.M., Pan, B.T., Su, H.**, 2020. Terraces development and their implications for valley evolution of the Jinsha River from Qiaojia to Menggu. [In Chinese with English abstract.] *Acta Geographica Sinica* **75**, 1095–1105.
- Liu, J.H., Gong, Z.J., Luo, M., Peng, H.M., Guo, F.S., Zhong, B.Y.**, 2021. Study the effect of water content and its error on the precision of optical age results for sediments. [In Chinese with English abstract.] *Quaternary Sciences* **41**, 123–135.
- Liu, W.M., Cui, P., Ge, Y.G., Yi, Z.Y.**, 2018. Paleosols identified by rock magnetic properties indicate dam-outburst events of the Min River, eastern Tibetan Plateau. *Palaeogeography, Palaeoclimatology, Palaeoecology* **508**, 139–147.
- Liu, Y., Wang, S.J., Xu, S., Fabel, D., Stuart, F.M., Rodés, A., Zhang, X.B., Luo, W.J.**, 2022. New chronological constraints on the Plio-Pleistocene uplift of the Guizhou Plateau, SE margin of the Tibetan Plateau. *Quaternary Geochronology* **67**, 101237. <https://doi.org/10.1016/j.quageo.2021.101237>.
- Liu, Y.M.**, 2020. Neogene fluvial sediments in the northern Jinshaan Gorge, China: implications for early development of the Yellow River since 8 Ma and its response to rapid subsidence of the Weihe-Shanxi Graben. *Palaeogeography, Palaeoclimatology, Palaeoecology* **546**, 109675. <https://doi.org/10.1016/j.palaeo.2020.109675>.
- Liu, Y.M., Rui, X.L., Li, Y.L.**, 2022. Long-term development archive of the Yellow River since the Neogene in the central Jinshaan Gorge, China. *Palaeogeography, Palaeoclimatology, Palaeoecology* **591**, 110899. <https://doi.org/10.1016/j.palaeo.2022.110899>.
- Long, Z.R., Wang, Z.B., Tu, H., Li, R.H., Wen, Z.H., Wang, Y.X., Zhang, Y., Lai, Z.P.**, 2022. OSL and radiocarbon dating of a core from the Bohai Sea in China and implication for Late Quaternary transgression pattern. *Quaternary Geochronology* **70**, 101308. <https://doi.org/10.1016/j.quageo.2022.101308>.
- Maddy, D., Veldkamp, A., Demir, T., Aytay, A.S., Lievens, C.**, 2020. Early Pleistocene river terraces of the Gediz River, Turkey: the role of faulting, fracturing, volcanism and travertines in their genesis. *Geomorphology* **358**, 107102. <https://doi.org/10.1016/j.geomorph.2020.107102>.
- Mischke, S., Lai, Z.P., Aichner, B., Heinecke, L., Mahmudov, Z., Kuessner, M., Herzschuh, U.**, 2017. Radiocarbon and optically stimulated luminescence dating of sediments from Lake Karakul, Tajikistan. *Quaternary Geochronology* **41**, 51–61.
- Nie, Y.P.**, 1994. Analysis to the trend surface of karst landform process in Mid-Southern Guizhou Province. [In Chinese with English abstract.] *Journal of Nanjing University (Natural Sciences Edition)* **30**, 154–159.
- Olszak, J.**, 2017. Climatically controlled terrace staircases in uplifting mountainous areas. *Global and Planetary Change* **156**, 13–23.
- Pan, B.T., Burbank, D., Wang, Y.X., Wu, G.J., Li, J.J., Guan, Q.Y.**, 2003. A 900 k.y. record of strath terrace formation during glacial-interglacial transitions in northwest China. *Geology* **31**, 957–960.
- Pan, B.T., Hu, Z.B., Wang, J.P., Vandenberghe, J., Hu, X.F., Wen, Y.H., Li, Q., Cao, B.**, 2012. The approximate age of the planation surface and the incision of the Yellow River. *Palaeogeography, Palaeoclimatology, Palaeoecology* **356–357**, 54–61.
- Pan, B.T., Su, H., Hu, Z.B., Hu, X.F., Gao, H.S., Li, J.J., Kirby, E.**, 2009. Evaluating the role of climate and tectonics during non-steady incision of the Yellow River: evidence from a 1.24 Ma terrace record near Lanzhou, China. *Quaternary Science Reviews* **28**, 3281–3290.
- Prescott, J.R., Hutton, J.T.**, 1994. Cosmic ray contributions to dose rates for luminescence and ESR dating: large depths and long-term time variations. *Radiation Measurements* **2–3**, 497–500.
- Qin, S.R., Zhang, H., Wang, T.H.**, 2002. Multi-grade planation surface of denudation in Guizhou. [In Chinese with English abstract.] *Guizhou Geology* **19**, 86–92.
- Ren, Z.S.**, 2019. Development of Fluvial Terraces in the Middle Reaches of the Yuanjiang River and its Response to Climate and Neotectonic Movement. [In Chinese.] Master's thesis, China University of Geosciences (Beijing), Beijing.
- Schanz, S.A., Montgomery, D.R., Collins, B.D., Duvall, A.R.**, 2018. Multiple paths to straths: a review and reassessment of terrace genesis. *Geomorphology* **312**, 12–23.

- Shen, Q.J., Ao, S.R.N., Xu, Y.T., Liu, S.W., Wang, Y.X., Lai, Y.S., Miao, X.D., Lai, Z.P., 2022. Aeolian landform processes since the last deglaciation revealed by OSL chronology and stratigraphy in the Hulunbuir dune field in NE China. *Quaternary Geochronology* **72**, 101352. <https://doi.org/10.1016/j.quageo.2022.101352>.
- Starkel, L., 2003. Climatically controlled terraces in uplifting mountain areas. *Quaternary Science Reviews* **22**, 2189–2198.
- Su, H., Dong, M., Hu, Z.B., 2019. Late Miocene birth of the Middle Jinsha River revealed by the fluvial incision rate. *Global and Planetary Change* **183**, 103002. <https://doi.org/10.1016/j.gloplacha.2019.103002>.
- Wang, B.L., Wang, X.Y., Yi, S.W., Zhao, L., Lu, H.Y., 2021. Responses of fluvial terrace formation to monsoon climate changes in the north-eastern Tibetan Plateau: evidence from pollen and sedimentary records. *Palaeogeography, Palaeoclimatology, Palaeoecology* **564**, 110196. <https://doi.org/10.1016/j.palaeo.2020.110196>.
- Wang, S.J., Zhang, X.B., Bai, X.Y., 2015. An outline of karst geomorphology zoning in the karst areas of Southern China. [In Chinese with English abstract.] *Mountain Research* **33**, 641–648.
- Wu, C., Li, J., Zuza, A.V., Liu, C.F., Liu, W.C., Chen, X.H., Jiang, T., Li, B., 2020. Cenozoic cooling history and fluvial terrace development of the western domain of the Eastern Kunlun Range, northern Tibet. *Palaeogeography, Palaeoclimatology, Palaeoecology* **560**, 109971. <https://doi.org/10.1016/j.palaeo.2020.109971>.
- Wu, D.Y., Li, B.J., Lu, H.H., Zhao, J.X., Zheng, X.M., Li, Y.L., 2020. Spatial variations of river incision rate in the northern Chinese Tian Shan range derived from late Quaternary fluvial terraces. *Global and Planetary Change* **185**, 103082. <https://doi.org/10.1016/j.gloplacha.2019.103082>.
- Xu, S., Liu, C.Q., Stewart, F., Lang, Y.C., Schnabei, C., Tu, C.L., Wilcken, K., Zhan, Z.Q., 2013. In-situ cosmogenic ^{36}Cl denudation rates of carbonates in Guizhou karst area. *Chinese Science Bulletin* **58**, 2473–2479.
- Yang, G.F., Zhang, X.J., Tian, M.Z., Brierley, G., Chen, A.Z., Ping, Y.M., Ge, Z.L., Ni, Z.Y., Yang, Z., 2011. Alluvial terrace systems in Zhangjiajie of northwest Hunan, China: implications for climatic change, tectonic uplift and geomorphic evolution. *Quaternary International* **233**, 27–39.
- Yang, H.J., 1944. The longitudinal and transverse profiles of the Maotiao River and their bearing on the morphological development of Central Kweichow. [In Chinese with English abstract.] *Acta Geographica Sinica* **11**, 1–14.
- Yang, Y., Lang, Y.C., Xu, S., Liu, C.Q., Cui, L.F., Freeman, S., Wilcken, K., 2020. Combined unsteady denudation and climatic gradient factors constrain carbonate landscape evolution: new insights from in situ cosmogenic ^{36}Cl . *Quaternary Geochronology* **58**, 101075. <https://doi.org/10.1016/j.quageo.2020.101075>.
- Yang, Y., Liu, C.Q., Vanderwoerd, J., Xu, S., Cui, L.F., Zhao, Z.Q., Wang, Q.L., Jia, G.D., Chabaux, F., 2019. New constraints on the late Quaternary landscape evolution of the eastern Tibetan Plateau from ^{10}Be and ^{26}Al in-situ cosmogenic nuclides. *Quaternary Science Reviews* **220**, 244–262.
- Yang, Y., Liu, Y., Ma, Y., Xu, S., Liu, C.Q., Wang, S.J., Stuart, F.M., Fabel, D., 2021. In situ cosmogenic ^{10}Be , ^{26}Al and ^{21}Ne dating in sediments from the Guizhou Plateau, southwest China. *Science China Earth Sciences* **64**, 1305–1317.
- Yuan, J.Y., Wu, Z.L., Yang, M.G., Zhao, H.T., 1988. A preliminary study on the terraces along the lower reaches of Beijiang, Suijiang and Xijiang rivers. [In Chinese with English abstract.] *Tropical Geography* **8**, 118–124.
- Zachos, J., Pagani, M., Sloan, L., Thomas, E., Billups, K., 2001. Trends, rhythms, and aberrations in global climate 65 Ma to present. *Science* **292**, 686–693.
- Zhang, J.F., Qiu, W.L., Li, R.Q., Zhou, L.P., 2009. The evolution of a terrace sequence along the Yellow River (HuangHe) in Hequ, Shanxi, China, as inferred from optical dating. *Geomorphology* **109**, 54–65.
- Zhou, D.Q., Liu, X.M., Jiang, L.J., Liu, C.R., 2005. Step-like landforms and uplift of Guizhou Plateau. [In Chinese with English abstract.] *Earth & Environment* **33**, 79–84.
- Zhou, Z.F., Zhang, S.Y., Xiong, K.N., Li, B., Tian, Z.H., Chen, Q., Yan, L.H., Xiao, S.Z., 2017. The spatial distribution and factors affecting karst cave development in Guizhou Province. *Journal of Geographical Sciences* **27**, 1011–1024.